Available online at www.sciencedirect.com

ScienceDirect

Advances in Space Research 72 (2023) 1070–1080

ADVANCES IN SPACE RESEARCH (a COSPAR publication)

www.elsevier.com/locate/asr

Absolute and relative POD of LEO satellites in formation flying: Undifferenced and uncombined approach

Xiaolong Mi [a], Amir Allahvirdi-Zadeh [a], Ahmed El-Mowafy [a], Zhiyong Huang [c], Kan Wang [d,e], Baocheng Zhang [b,f,*], Yunbin Yuan [b]

[a] School of Earth and Planetary Sciences, Curtin University, Perth, Australia
[b] State Key Laboratory of Geodesy and Earth's Dynamics, Innovation Academy for Precision Measurement Science and Technology, Chinese Academy of Sciences, Wuhan, China
[c] Institute of Geospatial Information, Information Engineering University, China
[d] National Time Service Center, Chinese Academy of Sciences, Xi'an, China
[e] University of Chinese Academy of Sciences, Beijing, China
[f] State Key Laboratory of Satellite Navigation System and Equipment Technology, the 54th Research Institute of China Electronics Technology Group Corporation, Shijiazhuang 050081, China

Received 7 February 2023; received in revised form 9 May 2023; accepted 13 May 2023
Available online 19 May 2023

Abstract

Absolute or relative precise orbit determination (POD) is an essential prerequisite for many low earth orbit (LEO) missions. The POD of LEO satellites typically relays on processing the onboard global navigation satellite system (GNSS) measurements. The absolute POD is usually based on an ionosphere-free (IF) combination, and currently, integer ambiguity resolution (IAR) can be achieved only when external GNSS satellite phase bias (SPB) products are used. The use of these products is not flexible in multi-frequency/multi-constella tion scenarios and is difficult to achieve in real-time missions. For relative POD, the double-differenced (DD) with IAR is the most general method. However, the differencing process amplifies observation noise and loses the opportunity to impose dynamic constraints on some eliminated parameters. In this contribution, based on the use of undifferenced and uncombined (UDUC) observations, a new model for both absolute and relative POD is proposed. In this model, the ambiguities of common-view satellites are constructed into DD form, thus IAR can be achieved without any external SPB products. Working with the UDUC observations, multi-frequency scenarios can be easily applied, and residuals can be separated for each frequency. In addition, with precise GNSS satellite clock/orbit products, both the absolute and relative orbits can be derived, which supports absolute and relative LEO POD. Based on onboard GPS observations of T-A and T-B satellites in formation flying, the performance of the UDUC POD model with DD ambiguity was evaluated. With the UDUC algorithm and IAR, the proposed model presented a consistency of 2.8–3.8 cm in 3D with the reference orbits, and the orbit difference was reduced by 16.3% and 10.6% for T-A and T-B compared with the IF-based POD, respectively. In addition, the relative orbit of the two satellites derived from the proposed model showed a consistency of 1.1–1.5 mm, which proved the feasibility of the UDUC POD model with DD ambiguity for formation flying missions.

Keywords: Low Earth Orbit (LEO); Precise Orbit Determination (POD); Formation flying; Global Navigation Satellite System (GNSS); Integer Ambiguity Resolution (IAR); Undifferenced and Uncombined (UDUC)

* Corresponding author.
E-mail addresses: xiaolong_mi@asch.whigg.ac.cn (X. Mi), amir.allahvirdizadeh@curtin.edu.au (A. Allahvirdi-Zadeh), A.El-Mowafy@curtin.edu.au (A. El-Mowafy), geo_hzy@126.com (Z. Huang), wangkan@ntsc.ac.cn (K. Wang), b.zhang@whigg.ac.cn (B. Zhang), yybgps@whigg.ac.cn (Y. Yuan).

https://doi.org/10.1016/j.asr.2023.05.024
0273-1177/

1. Introduction

Low Earth Orbit (LEO) satellites are those with orbital altitudes generally between a few hundred kilometers and 1500 km, which enables earth and space exploration with high-precision and high spatial–temporal resolution. Accurate orbital information in an absolute or relative mode is an essential prerequisite for many LEO missions (Montenbruck et al., 2009; Bandyopadhyay et al., 2016). The global navigation satellite system (GNSS) and the dynamics of LEO satellites have been used in the precise orbit determination (POD) algorithms. The kinematic and reduced-dynamic approaches are the two main POD methods developed during the past decades (Allahvirdi-Zadeh et al., 2021a, Allende-Alba et al., 2017; Montenbruck et al., 2018; Yunck et al., 1994). Compared to the reduced-dynamic method which exploits extensive dynamic models to estimate orbit perturbations, the kinematic POD is based on precise positioning using GNSS observations without considering any dynamic model (Allahvirdi-Zadeh et al., 2021b; Li et al., 2019c). Currently, there are several hundreds of LEO satellites, including nanosatellites and CubeSats flying in the LEO region. This number will increase in the coming years with more satellites launched for, e.g., aiding GNSS in Positioning, Navigation, and Timing (PNT) applications (Li et al., 2019a; Li et al., 2019b; El-Mowafy et al., 2022). In this sense, absolute and relative POD of LEO constellations are particularly essential mainly in (near) real-time.

Due to the introduction of precise satellite orbit and clock products, kinematic POD uses the concept of precise point positioning (PPP) (Bertiger et al, 2010; Zumberge et al., 1997) to obtain the state solution of a single LEO satellite. It is widely used in the absolute POD of LEO satellites (Hauschild et al., 2016), mainly when the orbits are required to not be affected by dynamic models. However, general kinematic POD usually utilizes the ionosphere-free (IF) combination, which has three disadvantages. Firstly, the IF combination causes a waste of observation information as only one independent parameter is eliminated at the expense of using more observational information (Teunissen, 2020). Secondly, as we explain in the paper, it is not conducive to the expansion of multi-frequency scenarios (Odijk et al., 2016). Thirdly, the ambiguities lose their integer characteristic in the IF model, which is not restored unless by applying external corrections, and limits the performance of the LEO POD. The integer ambiguity resolution (IAR) is needed for realizing high-precision GNSS positioning (Teunissen, 2001). There are some methods to achieve the POD with IAR, which are mainly based on the use of external satellite phase bias (SPB) products (Laurichesse et al., 2009; Ge et al., 2008; Collins, 2008). However, these methods are still based on the IF combination and are thus limited by its drawbacks (Odijk et al., 2016; Teunissen and Khodabandeh, 2015).

In addition to the absolute POD, accurate knowledge of relative states (position and velocity) and the baselines between LEO satellites are required in formation flying missions, as well as docking and rendezvous in space (Bandyopadhyay et al., 2016; Gill et al., 2007). To achieve high-precision relative state solutions, the double-differenced (DD) model with IAR is favored to remove highly correlated parameters and recover the integer nature of the ambiguities (Jäggi et al., 2012; Yi et al., 2022). However, this approach also has some drawbacks. Firstly, the DD model requires strict common-view satellites, which is not guaranteed for high-speed LEO satellites flying at different altitudes in the complex space environment. Secondly, the assumption of the differencing is that the eliminated parameters, such as receiver biases, do not have any time links (Zhang et al., 2019; Odijk et al., 2017). However, this is not the case in actual scenarios (Allahvirdi-Zadeh et al., 2022). The differencing process thus loses the opportunity to impose dynamic constraints on the eliminated parameters (Zhang et al., 2022). Thirdly, the noise of the DD observations is doubled compared to the original observations, which is unfavorable for high-precision relative navigation in formation flying missions, and this has to be considered when modelling their stochastic properties, e.g. in their covariance matrices. There are some remedies for these drawbacks that are implemented for the real-time kinematic (RTK) positioning application on the ground by constructing a single-differenced (SD) model using the *S*-system theory (Odolinski et al., 2015b; Mi et al., 2019). In this case, the stability of the receiver code and phase biases can be used to increase the strength of the model (Mi et al., 2020). However, the SD model still ignores the stability of code and phase biases at the GNSS end. In addition, the observation noise is amplified during the construction of the SD model compared to the undifferenced (UD) observations.

An alternative approach for the GNSS positioning is based on the undifferenced and uncombined (UDUC) GNSS observation equations (Zhang et al., 2011). In the UDUC approach, neither (single or double) differences are taken nor combinations are formed in the observation domain (Teunissen and Khodabandeh, 2015). The advantages of UDUC formulation have been recognized in geodesy and GNSS for a long time (Lindlohr and Wells, 1985; De Jonge, 1998; Lannes and Prieur, 2013). With uncombined formulation, one can extend the observation equations to arbitrary frequencies, and the ionospheric delays also remain in the observation equations, which can be estimated for use in environmental studies (Zha et al., 2021). Working with the undifferenced formulation allows all the parameters (after necessary re-formulation) to remain available for possible further model strengthening (Khodabandeh and Teunissen, 2015; Psychas et al., 2022). In addition, the UDUC observation equations allow the use of the simplest variance matrix without amplifying the observation noise. However, rank deficiencies need to be considered in the UDUC observation equations since the unbiased estimation of all parameters is impossible (Teunissen, 1985). The application of UDUC method in

LEO POD has been initially explored and has demonstrated its superiority compared with existing methods in various studies (Zehentner and Mayer-Gürr 2016; Suesser-Rechberger et al., 2022).

In this contribution, a new POD model based on the UDUC observations is developed. After removing the rank deficiencies, the ambiguities are presented in the DD form to facilitate the IAR. With the introduction of precise GNSS satellite orbit and clock products, both absolute and relative POD can be achieved using the proposed model. The paper aims to study the benefits of the UDUC formulation and IAR for both absolute and relative POD. In the next section, the UDUC POD model with DD ambiguity is first developed. Next, the proposed model is verified using T-A and T-B LEO satellites in both absolute and relative POD cases. In the last section, the findings are summarized and the conclusions are given.

2. Methodology

In this section, based on the raw GNSS observations, a full-rank UDUC POD model with DD ambiguity will be constructed with the application of the *S*-system theory (Teunissen 1985; Odijk et al., 2016). It will be shown how the model applies to the absolute and relative POD of LEO satellites.

2.1. UDUC GNSS observation equations for LEO satellite

As the starting point of developing the model, we first give the equations for raw GNSS code and phase observations of the LEO satellite, which read,

$$\begin{aligned} p^s_{r,j} &= \rho^s_r + dt_r - dt^s + \mu_j I^s_r + d_{r,j} - d^s_{,j} + \varepsilon^s_{p,j} \\ \phi^s_{r,j} &= \rho^s_r + dt_r - dt^s - \mu_j I^s_r + \lambda_j N^s_{r,j} + \delta_{r,j} - \delta^s_{,j} + \varepsilon^s_{\phi,j} \end{aligned} \tag{1}$$

where $p^s_{r,j}$ and $\phi^s_{r,j}$ are the raw code and phase observables with GNSS satellite s, LEO satellite r and frequency j, respectively.ρ^s_r is the GNSS-LEO satellite range, which includes the antenna calibration of phase center offset (PCO) and variations (PCV) for code and phase, and phase wind up for the phase. dt_r and dt^s are the LEO and GNSS satellite clock offsets, respectively.I^s_r and $\mu_j = \lambda_j^2/\lambda_1^2$($\lambda_j$ is the wavelength of frequency j) are the ionospheric delay on the first frequency and its coefficient.$N^s_{r,j}$ is the phase ambiguity. $d_{r,j}$ and $d^s_{,j}$ are the LEO and GNSS satellite code biases, respectively, and their counterpart $\delta_{r,j}$ and $\delta^s_{,j}$ are the LEO and GNSS satellite phase biases. $\varepsilon^s_{p,j}$ and $\varepsilon^s_{\phi,j}$ denote the code and phase observation noises and miss-modeled effects including multipath.

2.2. Uncombined (UC) POD model

Due to the existence of the following rank deficiencies, the unknowns in Eq. (1) are difficult to be estimated individually. Therefore, as the first step in constructing the full-rank model, it is necessary to identify these rank deficiencies using the *S*-system theory. With m GNSS satellites and f frequencies tracked at each epoch, eight types of rank deficiencies with one LEO satellite are identified (Odijk et al., 2016; Mi et al. 2023), in the corresponding class:

1. Between the LEO and GNSS satellite clocks of size 1;
2. Between the LEO and GNSS satellite code biases of size f;
3. Between the LEO and GNSS satellite phase biases of size f;
4. Between the LEO satellite clock, code biases and phase biases of size 1;
5. Between the GNSS satellite clocks, code biases and phase biases of size m;
6. Between the GNSS satellite phase biases and ambiguities of size $f \times m$;
7. Between the ionospheric delays, LEO satellite code and phase biases of size 1;
8. Between the ionospheric delays, GNSS satellite code and phase biases of size m.

where the size means the number of rank deficiencies.

Let's review how the classical IF model for the kinematic POD is formed from Eq. (1) and what are the drawbacks of such a model. To achieve precise kinematic POD of LEO satellites, precise GNSS satellite orbits and clocks are necessary. When using precise satellite clock products, the rank deficiencies of types 1 and 5 no longer exist. $\tilde{dt}^s = dt^s + d^s_{,IF}$ is the precise satellite clock provided by the International GNSS Service (IGS), where $d^s_{,IF} = \frac{\mu_2}{\mu_2-\mu_1} d^s_{,1} - \frac{\mu_1}{\mu_2-\mu_1} d^s_{,2}$. For classical PPP based on the IF combination, the seventh and eighth types of rank deficiencies do not need to be considered either. After solving the remaining four rank deficiencies (No. 2, 3, 4, and 6), the full-rank model of the IF POD model can be expressed as:

$$\begin{aligned} \tilde{p}^s_{r,IF} &= \rho^s_{r,j} + \tilde{dt}_r + \varepsilon^s_{p,IF} \\ \tilde{\phi}^s_{r,IF} &= \rho^s_{r,j} + \tilde{dt}_r - \tilde{\delta}^s_{r,IF} + \varepsilon^s_{\phi,IF} \end{aligned} \tag{2}$$

where $\tilde{p}^s_{r,IF} = p^s_{r,IF} + \tilde{dt}^s$ and $\tilde{\phi}^s_{r,IF} = \phi^s_{r,IF} + \tilde{dt}^s$, respectively. $\tilde{dt}_r = dt_r + d_{r,IF}$ is the estimable LEO satellite clock offset, where $d_{r,IF}$ is the IF LEO code bias. $\tilde{\delta}^s_{r,IF} = \delta_{r,IF} - \delta^s_{,IF} - d_{r,IF} + \lambda_{IF} N^s_{r,IF}$ is the estimable phase ambiguity. As presented in Eq. (2), although the ionospheric delays are eliminated, the observational noise is amplified at the same time. Taking the dual-frequency case as an example, the IF combination is formed in code and phase observations, respectively, but only an independent parameter of the ionosphere delay is eliminated, resulting in a waste of observational information. This is critical for the onboard receivers with a limited number of channels tracking GNSS satellites. In addition, in multi-frequency scenarios, multiple IF combinations can be formed, but this approach has two drawbacks. The first

is wasting observational information, and the second is obscuring the possible correlations between the combined observations (Teunissen, 2020). Therefore, the IF combination is not the optimal choice for multi-frequency multi-constellation GNSS data processing.

To provide a solution to such limitations, we form the full-rank model for the UC observation (Zha et al., 2021). With precise satellite clock products, we are free from the first and the fifth types of rank deficiency. These deficiency types are described in the section "***Uncombined (UC) POD model***" in the paper. To address the second and the third types of rank deficiency, the LEO code biases ($d_{r,j}$) and phase biases ($\delta_{r,j}$) are chosen as the *S*-basis, respectively. The rank deficiency (of size 1) between the LEO satellite clock, code biases and phase biases can be eliminated by fixing the IF code bias of the LEO satellite as an *S*-basis. For the rank deficiencies between the ionospheric delays, LEO satellite code and phase biases and between the ionospheric delays, GNSS satellite code and phase biases are usually eliminated by fixing the geometry-free (GF) code bias of the LEO satellite and GNSS satellite as the *S*-basis, respectively. After solving those rank deficiencies, the full-rank UC POD model can be expressed as (Zehentner and Mayer-Gürr, 2016),

$$\begin{aligned}\tilde{p}{}^{s}_{r,j} &= \rho^{s}_{r} + \tilde{dt}_{r} + \mu_j \tilde{I}{}^{s}_{r} - \tilde{d}{}^{s}_{r,j} + \varepsilon^{s}_{p,j} \\ \overset{\sim}{\phi}{}^{s}_{r,j} &= \rho^{s}_{r} + \tilde{dt}_{r} - \mu_j \tilde{I}{}^{s}_{r} - \overset{\sim}{\delta}{}^{s}_{r,j} + \varepsilon^{s}_{\phi,j}\end{aligned} \tag{3}$$

where $\tilde{p}{}^{s}_{r,j} = p^{s}_{r,j} + \tilde{dt}^{s}$ and $\overset{\sim}{\phi}{}^{s}_{r,j} = \phi^{s}_{r,j} + \tilde{dt}^{s}$ are code and phase observables with satellite clock corrected.$\tilde{I}{}^{s}_{r} = I^{s}_{r} + d_{r,GF} - d^{s}_{,GF}$ is the estimable ionospheric delay. $d_{r,GF} = \frac{1}{\mu_2-\mu_1}(d_{r,2} - d_{r,1})$ and $d^{s}_{,GF} = \frac{1}{\mu_2-\mu_1}(d^{s}_{,2} - d^{s}_{,1})$ denote the GF code bias of LEO and GNSS satellites, respectively. $\tilde{d}{}^{s}_{r,j} = d^{s}_{,j} - d^{s}_{,IF} - \mu_j d^{s}_{,GF} - d_{r,j} + d_{r,IF} + \mu_j d_{r,GF}$ is the combined GNSS and LEO satellite code bias with $j \geqslant 3$, which shows the flexibility of the UC POD model for multi-frequency expansion. $\overset{\sim}{\delta}{}^{s}_{r,j} = \delta^{s}_{,j} - d^{s}_{,IF} + \mu_j d^{s}_{,GF} - \lambda_j N^{s}_{r,j} - \delta_{r,j} + d_{r,IF} - \mu_j d_{r,GF}$ is the combined GNSS and LEO satellite phase bias, which also absorbs the ambiguity parameters. In addition, it can be seen from Eq. (3) that the UC POD model retains the original observation noise and facilitates the analysis of residuals at each frequency; something that is not possible for the IF POD model.

2.3. UDUC POD model with DD ambiguity

Concerning the absolute POD for LEO constellations, there are two points that cannot be ignored. First, the phase ambiguities are present in the float form in the UC POD model, which limits the POD performance. Second, the properties of the common-view GNSS satellites in the LEO constellation are ignored. With the help of these common-view satellites, the joint POD of the LEO constellation can be realized, which can improve computational efficiency compared with the satellite-by-satellite POD. In addition, DD ambiguities with integer characteristics can also be constructed with the help of the common-view satellites. In the relative POD, the DD model is widely used because the model does not have any rank deficiency. However, the DD model only obtains relative states and requires strict common-view GNSS satellites. Possible non-common-view satellite observations are wasted in such cases.

Considering the above points, we present here a model that can serve both the absolute and relative POD based on the UC POD model by taking advantage of the characteristics of common-view GNSS satellites. Satellites *A* and *B* are assumed in a LEO constellation, so that the model can be easily extended to other multi-satellite cases. For the common-view GNSS satellites, the satellite code and phase biases $d^{s}_{,j} - d^{s}_{,IF} - \mu_j d^{s}_{,GF}$ and $\delta^{s}_{,j} - d^{s}_{,IF} + \mu_j d^{s}_{,GF}$ are the same for the LEO satellites *A* and *B*. Taking $\tilde{d}{}^{s}_{A,j}$ and $\overset{\sim}{\delta}{}^{s}_{A,j}$ as the *S*-basis, the parameters to be estimated can be reduced. In addition, the ambiguities can be constructed in the DD form. In this case, the UDUC POD model with DD ambiguity can be constructed as follows,

$$\begin{aligned}\tilde{p}{}^{s}_{A,j} &= \rho^{s}_{A} + \tilde{dt}_{A} + \mu_j \tilde{I}{}^{s}_{A} - \tilde{d}{}^{s}_{A,j} + \varepsilon^{s}_{p,j} \\ \overset{\sim}{\phi}{}^{s}_{A,j} &= \rho^{s}_{A} + \tilde{dt}_{A} - \mu_j \tilde{I}{}^{s}_{A} - \overset{\sim}{\delta}{}^{s}_{A,j} + \varepsilon^{s}_{\phi,j} \\ \tilde{p}{}^{s}_{B,j} &= \rho^{s}_{B} + \tilde{dt}_{B} + \mu_j \tilde{I}{}^{s}_{B} - \tilde{d}{}^{s}_{A,j} + \tilde{d}_{AB,j} + \varepsilon^{s}_{p,j} \\ \overset{\sim}{\phi}{}^{s}_{B,j} &= \rho^{s}_{B} + \tilde{dt}_{B} - \mu_j \tilde{I}{}^{s}_{B} - \overset{\sim}{\delta}{}^{s}_{A,j} + \tilde{\delta}_{AB,j} + \lambda_j N^{1s}_{AB,j} + \varepsilon^{s}_{\phi,j}\end{aligned} \tag{4}$$

where $\tilde{d}_{AB,j} = d_{B,j} - d_{A,j} - d_{AB,IF} - \mu_j d_{AB,GF}$ is the between-LEO code bias when $j \geqslant 3$ and $\tilde{\delta}_{AB,j} = \delta_{B,j} - \delta_{A,j} - d_{AB,IF} + \mu_j d_{AB,GF} + \lambda_j N^{1}_{AB,j}$ is the between-LEO phase bias with $j \geqslant 1$. $N^{1s}_{AB,j} = N^{s}_{AB,j} - N^{1}_{AB,j}$ is the DD ambiguity. Kalman filter is used in the UDUC model with DD ambiguity, where $\tilde{d}_{AB,j}$,$\tilde{\delta}_{AB,j}$,$\tilde{d}{}^{s}_{A,j}$,$\overset{\sim}{\delta}{}^{s}_{A,j}$ and $N^{1s}_{AB,j}$ are estimated as time-invariant parameters.

The UDUC model with DD ambiguity has the following advantages:

1. The model can estimate the absolute orbit of each LEO satellite as well as the relative state between LEO satellites, thus can serve both absolute and relative POD.
2. The ambiguities are in the DD form, thus IAR can be performed without external SPB products.
3. Joint POD of a LEO constellation reduces the number of estimated parameters, which can improve computational efficiency.
4. Code and phase biases at both LEO and GNSS-end remained for further model strengthening.
5. For those GNSS satellites which are non-common-view, they also contribute to POD with the UC POD model.

The model, however, has two extreme cases. Firstly, when the distance between the LEO satellites is long such that there are no common-view GNSS satellites at all, this will be equivalent to having two LEO satellites performing the UC POD model separately. Although this method can be applied to long baselines in theory, it might be difficult to solve the IAR due to the length of the baseline being too long in practice, which will affect the accuracy of the POD. Secondly, when the common-view GNSS satellites of the two LEO satellites are the same, which is equivalent to the relative POD based on the UD model. It should be mentioned that in the second case, the UD model also has advantages over the traditional DD model since it can better utilize the stability of LEO and GNSS satellite biases to improve the model strength.

Eq. (4) can be defined as the ionosphere-float UDUC POD model with DD ambiguity, as no constraint is assumed between I^s_A and I^s_B in this situation. However, when the distance between the two LEO satellites in formation flying is between 10 km and 200 km, the model strength can be improved by imposing SD ionospheric constraints with pseudo-observables (Odijk, 2000; Odijk, 2002). Adding those observables enables a-priori reasonable information on the ionospheric delay. In this case, the ionosphere-weighted UDUC POD model with DD ambiguity can be constructed as follow,

$$\begin{aligned}
\tilde{p}^s_{A,j} &= \rho^s_A + \tilde{dt}_A + \mu_j \tilde{I}^s_A - \tilde{d}^s_{A,j} + \varepsilon^s_{p,j} \\
\tilde{\phi}^s_{A,j} &= \rho^s_A + \tilde{dt}_A - \mu_j \tilde{I}^s_A - \tilde{\delta}^s_{A,j} + \varepsilon^s_{\phi,j} \\
\tilde{p}^s_{B,j} &= \rho^s_B + \tilde{dt}_B + \mu_j \tilde{I}^s_A + \mu_j I^s_{AB} + \mu_j d_{AB,GF} - \tilde{d}^s_{A,j} + \tilde{d}_{AB,j} + \varepsilon^s_{p,j} \\
\tilde{\phi}^s_{B,j} &= \rho^s_B + \tilde{dt}_B - \mu_j \tilde{I}^s_A - \mu_j I^s_{AB} - \mu_j d_{AB,GF} - \tilde{\delta}^s_{A,j} + \tilde{\delta}_{AB,j} + \lambda_j N^{1s}_{AB,j} \\
&\quad + \varepsilon^s_{\phi,j} \\
\bar{I}^s_{AB} &= I^s_{AB} + \varepsilon^s_{AB}
\end{aligned} \tag{5}$$

where $\bar{I}^s_{AB}$ and I^s_{AB} is the between-LEO SD ionospheric delay and its pseudo-observables. ε^s_{AB} is the random observation noise of the between-LEO SD ionospheric delay. With the between-LEO differential code biases (DCB) $d_{AB,GF}$, the ionospheric delay of LEO satellite B does not need to be estimated in the model, consequently, the model strength improves.

In addition, if the distance between LEO satellites is less than 10 km, it is safe to assume $I^s_{AB} = 0$ (Odolinski et al., 2015a). Thus, the ionosphere-fixed UDUC POD model with DD ambiguity can be written as,

$$\begin{aligned}
\tilde{p}^s_{A,j} &= \rho^s_A + \tilde{dt}_A + \mu_j \tilde{I}^s_A - \tilde{d}^s_{A,j} + \varepsilon^s_{p,j} \\
\tilde{\phi}^s_{A,j} &= \rho^s_A + \tilde{dt}_A - \mu_j \tilde{I}^s_A - \tilde{\delta}^s_{A,j} + \varepsilon^s_{\phi,j} \\
\tilde{p}^s_{B,j} &= \rho^s_B + \tilde{dt}_B + \mu_j \tilde{I}^s_A + \mu_j d_{AB,GF} - \tilde{d}^s_{A,j} + \tilde{d}_{AB,j} + \varepsilon^s_{p,j} \\
\tilde{\phi}^s_{B,j} &= \rho^s_B + \tilde{dt}_B - \mu_j \tilde{I}^s_A - \mu_j d_{AB,GF} - \tilde{\delta}^s_{A,j} + \tilde{\delta}_{AB,j} + \lambda_j N^{1s}_{AB,j} + \varepsilon^s_{\phi,j}
\end{aligned} \tag{6}$$

where the interpretation of the estimated parameters is the same as in Eq. (5).

3. Results

This section will first introduce the LEO satellites involved in this experiment. The data processing strategy of LEO will be given, and the results of absolute and relative POD will be shown on this basis.

3.1. LEO data and processing strategy

The satellites used in our experiments are two LEO satellites T-A and T-B, working in a formation flying (Lou et al., 2020). T-A and T-B orbit the Earth at 527 km altitude in an orbital plane with an inclination of 97.5°, completing one revolution in roughly 95 min (Yi et al., 2021a; Zhang et al., 2021). The relevant characteristics of the mission are summarized in Table 1.

To validate the feasibility and effectiveness of the UDUC POD model with DD ambiguity, we test using the onboard GPS data of T-A and T-B satellites from September 2nd to 8th, 2021. GPS L1 and L2 observations with a sampling rate of 10 s were used in our study. The IGS final precise GPS orbits and clocks products were used (Johnston et al., 2017), and GPS P1-C1 DCB was corrected using the monthly DCBs published by the Centre for Orbit Determination in Europe (CODE) (Dach et al., 2016). Considering that the distance between T-A and T-B is usually within two kilometers (Zhang et al., 2021), the ionosphere-fixed UDUC POD model with DD ambiguity was adopted. The main data processing strategies for the UDUC POD model with DD ambiguity are summarized in Table 2.

3.2. POD performance of the UDUC POD model with DD ambiguity

Comparing the orbit solutions with precise reference orbits is a simple and effective means of evaluating the LEO POD model. In this section, the kinematic orbits generated using the UDUC POD model with DD ambiguity are compared with the reference orbits provided courtesy of the operating team of the mission of T-A and T-B.

Table 1
An overview of the mission.

Item	Index
Satellites	T-A and T-B
Orbit	Sun-synchronous
Altitude	527 km
Inclination	97.5°
Period	95 min
GNSS system tracked	GPS and BDS-3
Measurement	Code, Phase and Doppler
Sample interval	1 s

Table 2
Main data processing strategies in the study.

Item	Strategy
Observation	GPS L1 + L2
GPS antenna offset	PCO and PCV are corrected with IGS igs14.atx (Rebischung and Schmid, 2016)
LEO antenna offset	PCO is corrected with the value from the data provider
LEO attitude	Quaternions from onboard star trackers
SPB	Estimated as time-constants in a continuous arc
Between-LEO phase biases	Estimated as time-constants
Between-LEO DCB	Estimated as a time-constant
Slant ionospheric delays	Estimated as white noise
Parameter estimator	Kalman filter
IAR and validation	LAMBDA (Teunissen, 1995) with ratio test (Verhagen and Teunissen, 2013)
Outlier detection and elimination	Detection, identification, and adaptation (DIA) procedure (Teunissen, 2018)

The reference orbits of the two satellites are generated using a reduced-dynamic model in post-processed batch least-squares adjustment. IAR is performed for the reference orbits with the SD method (Yi et al., 2021; Zhang et al., 2021). To show the performance improvement with the use of our model compared to the classical POD model, the orbits of the classical kinematic IF POD are calculated using Bernese GNSS software V5.4 (Dach and Walser 2015). The kinematic orbits generated by Bernese GNSS Software are ambiguity-fixed solutions using the phase bias products provided by the CODE (Schaer et al., 2021).

Fig. 1 shows the orbit differences of the kinematic IF POD and UDUC POD with DD ambiguity solutions for T-A with respect to the reference orbit on the day of year (DOY) 248 (September 5th), 2021. There is a gap in the results for nearly two hours due to multiple satellite maneuvers during this period with some orbital data missing. Compared with the IF POD, the orbits calculated by the UDUC POD with DD ambiguity are more consistent with the reference orbit. The root mean square (RMS) values of the orbit differences in three directions for the IF POD are 2.7 cm, 2.6 cm and 2.6 cm and that for the UDUC POD with DD ambiguity are 2.0 cm, 2.2 cm and 2.3 cm. The reduction of the orbit differences of the proposed model is thus 25.9%, 15.4% and 11.5% compared to the IF POD, respectively. The UDUC POD with DD ambiguity performs better than the IF POD for the following reasons. Firstly, IAR is achieved for the UDUC POD with DD ambiguity, which guarantees high-precision orbit solutions. Secondly, ionospheric constraints are considered in the UDUC POD with DD ambiguity, enabling instantaneous IAR to speed up the solution convergence process. Fig. 2 is analogous to Fig. 1 but illustrates the results for T-B. Unlike T-A, T-B does not have any maneuvers on this day. From the results, it can also be seen that the UDUC POD with DD ambiguity performs better than the IF

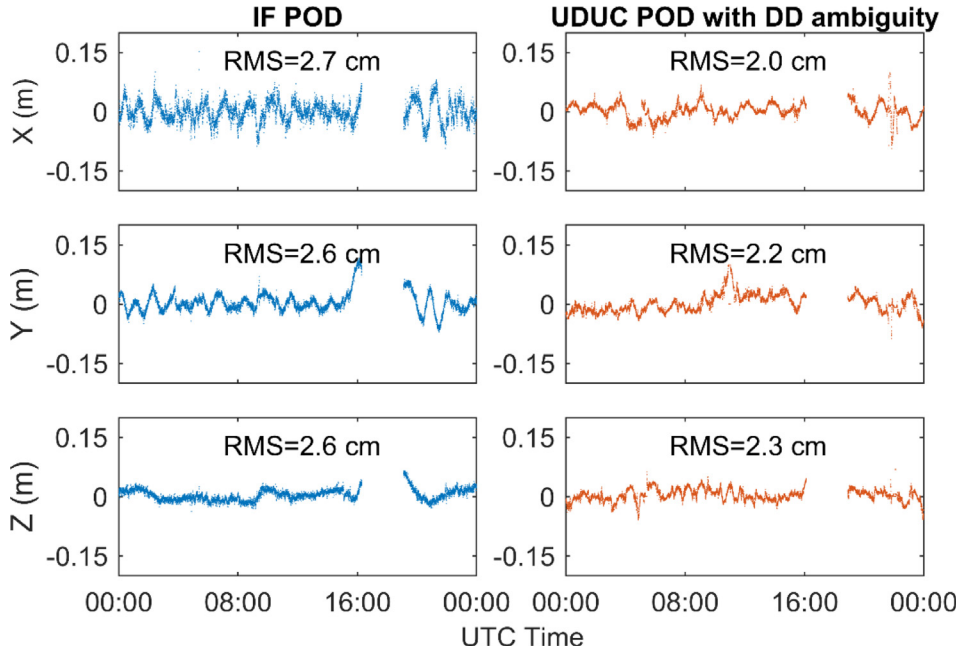

Fig. 1. Orbit differences of the IF POD and UDUC POD with DD ambiguity of T-A with respect to the reference orbit on DOY 248 (September 5th), 2021.

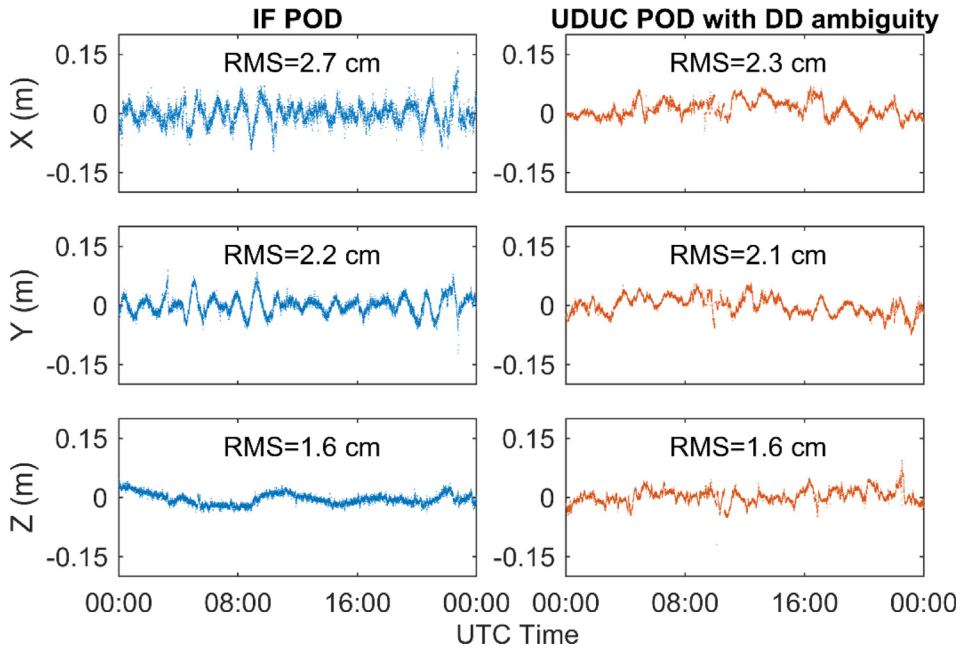

Fig. 2. Orbit differences of the IF POD and UDUC POD with DD ambiguity of T-B with respect to the reference orbit on DOY 248 (September 5th), 2021.

POD from the RMS of orbit differences with the reference orbit. The RMS of orbit differences for two models in three directions are 2.7 cm, 2.2 cm and 1.6 cm and 2.3 cm, 2.1 cm and 1.6 cm, respectively. Also note that the Bernese GNSS Software results in the left panel of Fig. 1 are processed based on batch least-squares adjustment, which can only be achieved in near-real-time due to the processing time of a few minutes up to more than 10 min, depending on the computational efficiency. The UDUC results from the right panel of Fig. 1 are processed with a Kalman filter, which can be achieved almost in real-time with much shorter delays.

The POD results of T-A and T-B covering one week in the test period are shown in Fig. 3 and Fig. 4 with box-whisker diagrams for the IF POD and UDUC POD with DD ambiguity. In a box-whiskers diagram, the maximum and minimum values are displayed. In addition, the first and third quartiles are indicated by the top and bottom edges of each box, while the median is marked as the centerline of the box. The RMS values of the orbit differences

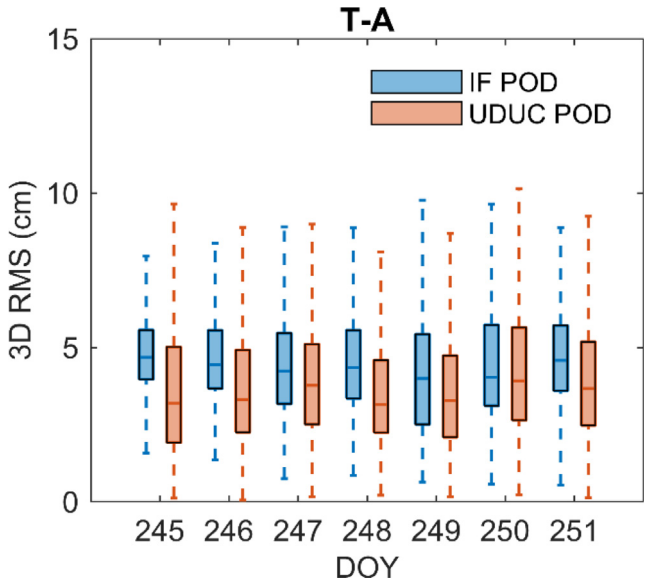

Fig. 3. Daily 3D RMS of orbit differences of the IF POD and UDUC POD with DD ambiguity with respect to the reference orbits for T-A on DOYs 245–251 (September 2nd to 8th), 2021.

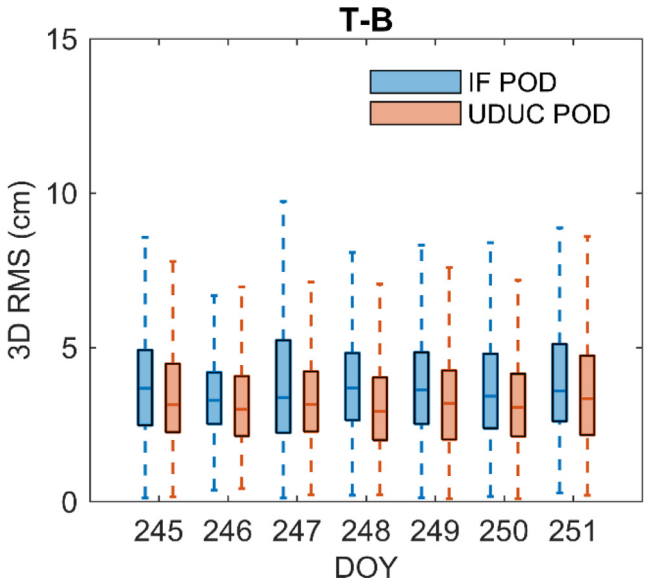

Fig. 4. Daily 3D RMS of orbit differences of the IF POD and UDUC POD with DD ambiguity with respect to the reference orbits for T-B on DOYs 245–251 (September 2nd to 8th), 2021.

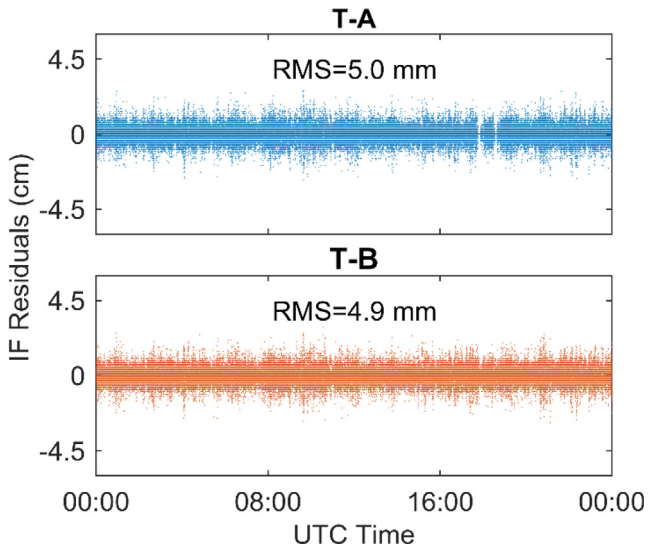

Fig. 5. IF phase residuals of the IF POD for T-A and T-B on DOY 247 (September 4th), 2021.

with respect to the reference orbit is displayed. The median absolute errors amount to between 3.4 cm and 4.6 cm for T-A with the IF POD. When using the UDUC POD with DD ambiguity, corresponding values of 2.9 cm to 3.8 cm were obtained for the testing period. For T-B, the median of the absolute errors of the IF POD are from 3.0 cm to 3.6 cm and of the UDUC POD with DD ambiguity are between 2.8 cm and 3.1 cm. The average percentage of reduction in the orbit differences in 3D of the proposed model is 16.3% and 10.6% for T-A and T-B, respectively, compared with the IF POD. This comparison verifies the advantages of the UDUC POD with DD ambiguity.

As an alternative indicator, phase residuals are usually used to assess the internal precision of orbit solutions. As we mentioned earlier, another advantage of the UDUC POD with DD ambiguity is that the original observation noise is preserved and the residuals at each frequency can be separated. However, the IF POD can only output the combined phase residuals and cannot distinguish the contributions of different frequencies. Take DOY 247, 2021 as an example, Fig. 5 presents the IF phase residuals of the IF POD. The phase residuals fluctuate randomly around the mean for both T-A and T-B. In addition, the RMS of IF phase residuals for T-A and T-B are 5.0 mm and 4.9 mm, respectively.

However, when the UDUC POD with DD ambiguity is used, the phase residuals of L1 and L2 can be separated. Fig. 6 shows the phase residuals of L1 and L2 separately for T-A and T-B, respectively, from which two conclusions can be drawn. Firstly, with the UDUC POD with DD ambiguity, smaller residuals can be obtained compared with the IF POD. Taking T-A as an example, the phase residuals for L1 and L2 are 1.8 mm and 1.7 mm, respectively, which is smaller than the IF residuals obtained from the IF POD. The reasons are as follows. Firstly, the original observation noise is preserved without amplification in the UDUC method. Secondly, the phase residuals are further reduced with successful IAR. In addition, for T-A and T-B, the phase residuals of L2 are always smaller than that of L1, which indicates that the L2 observations are more accurate than that of L1, hence, they can play an important role in POD.

With the UDUC POD with DD ambiguity, the orbits of each LEO satellite can be obtained. In addition, relative POD can also be achieved with this method. Fig. 7 depicts the results compared to the reference baseline for seven days. The reference baseline between T-A and T-B is generated based on the DD model with IAR. The median absolute errors amount to 1.1–1.5 mm in 3D for the week (September 2nd to 8th), respectively. The above results show that the UDUC POD with DD ambiguity can

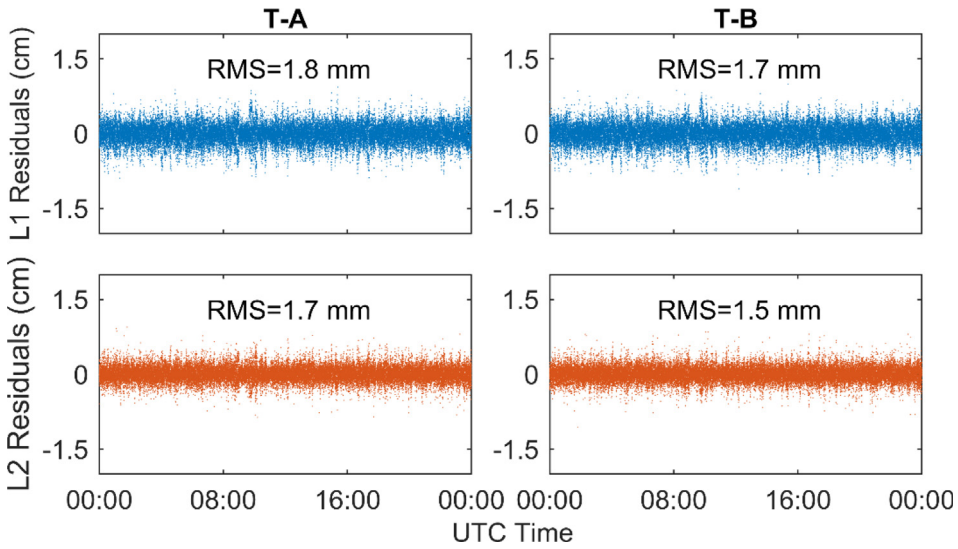

Fig. 6. L1 and L2 phase residuals of the UDUC POD with DD ambiguity for T-A and T-B on DOY 247 (September 4th), 2021.

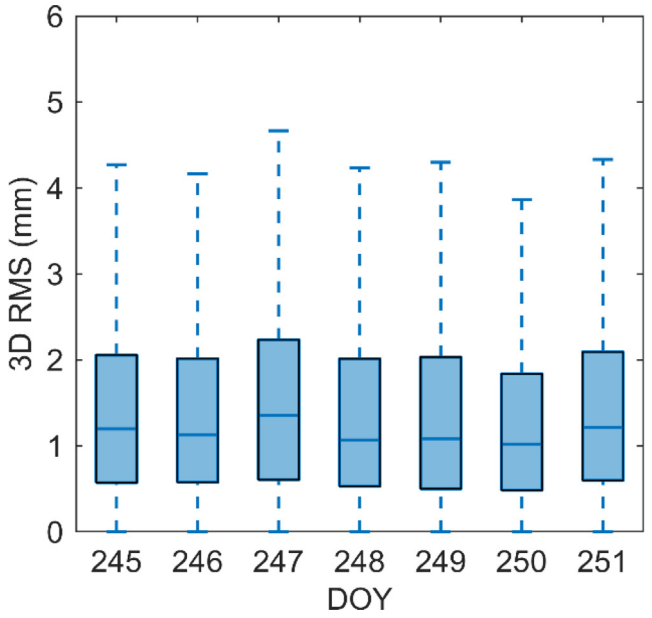

Fig. 7. 3D Differences of the baseline solutions between the UDUC POD with DD ambiguity and the reference for T-A and T-B on DOYs 245–251 (September 2nd to 8th), 2021.

achieve millimeter-level relative POD, which can be used for formation flying, space docking and rendezvous missions.

4. Conclusions

In this contribution, we developed a model based on the UDUC observations that can be used for absolute and relative LEO POD, namely the UDUC POD model with DD ambiguity. This model has the following characteristics, making it well-suited for different LEO satellite missions including formation flying:

1. The model is based on the UDUC observations, which can be flexibly used in multi-frequency scenarios and the original observation noise is not amplified as in the difference modes.
2. DD ambiguities are formed with common-view GNSS satellites, enabling IAR for high-precision LEO POD without any SPB products.
3. All the parameters, such as code and phase biases of LEO and GNSS satellites, remain available for possible further model strengthening.
4. With the use of precise products, the non-common-view GNSS satellites can also be used, and both absolute and relative POD can be achieved.
5. Phase residuals of each frequency can be separated, which is useful for exploring and analysing the contribution of observations with different frequencies.

Based on onboard GPS data from two LEO satellites for formation flying, the performance of the proposed UDUC POD model with DD ambiguity was evaluated. In addition, classical kinematic IF POD was generated to demonstrate the benefits of the proposed model. The orbits generated by the IF POD and the UDUC POD with DD ambiguity for the two LEO satellites were compared with the reference orbits. The experimental results showed that compared with the IF POD, the differences between the UDUC POD with DD ambiguity solution and the reference orbit were smaller. This result illustrates that the UDUC algorithms and IAR were beneficial for LEO POD. The phase residuals of L1 and L2 were obtained with the proposed model, which are much smaller than the IF phase residuals with the IF POD, which showed the advantages of the UDUC model with DD ambiguity. By comparing the computed distance from the estimated two LEO satellite positions with their reference baseline, the ability of the UDUC POD with DD ambiguity solution to achieve millimeter-level relative POD was demonstrated, proving that the model could be used for formation flying missions, as well as space docking and rendezvous applications.

This study shows the potential of the UDUC algorithms with IAR for absolute and relative LEO POD. The current research is only focused on onboard GPS observations without any dynamic modeling. However, if dynamic models can be introduced, the UDUC POD model with DD ambiguity will hopefully serve real-time LEO POD with IAR. Thus, our future work will consider the reduced-dynamic POD based on the use of this model.

Declaration of Competing Interest

The authors declare that they have no known competing financial interests or personal relationships that could have appeared to influence the work reported in this paper.

Acknowledgments

This work was partially funded by the Australian Research Council Discovery Project (Grant No. DP 190102444), the National Natural Science Foundation of China (Grant No. 42022025) and the National Time Service Center, Chinese Academy of Sciences (CAS) (No. E167SC14). Baocheng Zhang is supported by the CAS Pioneer Hundred Talents Program. We thank the IGS for providing precise orbit and clock products.

References

Allahvirdi-Zadeh, A., Wang, K., El-Mowafy, A., 2021a. POD of small LEO satellites based on precise real-time MADOCA and SBAS-aided PPP corrections. GPS Solut. 25, 1–14. https://doi.org/10.1007/s10291-020-01078-8.

Allahvirdi-Zadeh, A., Wang, K., El-Mowafy, A., 2021b. Precise orbit determination of LEO satellites based on undifferenced GNSS observations. J. Surv. Eng. 148 (1). https://doi.org/10.1061/(ASCE)SU.1943-5428.0000382 03121001.

Allahvirdi-Zadeh, A., Awange, J., El-Mowafy, A., Ding, T., Wang, K., 2022. Stability of CubeSat clocks and their impacts on GNSS radio occultation. Remote Sens. (Basel) 14 (2), 1–26. https://doi.org/10.3390/rs14020362.

Allende-Alba, G., Montenbruck, O., Jäggi, A., Arnold, D., Zangerl, F., 2017. Reduced-dynamic and kinematic baseline determination for the

Swarm mission. GPS Solut. 21, 1275–1284. https://doi.org/10.1007/s10291-017-0611-z.
Bandyopadhyay, S., Foust, R., Subramanian, G.P., Chung, S.J., Hadaegh, F.Y., 2016. Review of formation flying and constellation missions using nanosatellites. J. Spacecr. Rocket. 53 (3), 567–578. https://doi.org/10.2514/1.A33291.
Bertiger, W., Desai, S.D., Haines, B., Harvey, N., Moore, A.W., Owen, S., Weiss, J.P., 2010. Single receiver phase ambiguity resolution with GPS data. J. Geod. 84, 327–337. https://doi.org/10.1007/s00190-010-0371-9.
Collins, P., 2008. Isolating and estimating undifferenced GPS integer ambiguities. In Proceedings of the 2008 National Technical Meeting of The Institute of Navigation, (720-732).
Dach, R., Walser, P., 2015. Bernese GNSS Software Version 5.2. https://doi.org/10.7892/boris.72297.
Dach, R., Schaer, S., Arnold, D., Orliac, E., Prange, L., Susnik, A., Villiger, A., Jäggi, A., 2016. CODE final product series for the IGS. https://doi.org/10.7892/boris.75876.4
De Jonge, P.J., 1998. A processing strategy for the application of the GPS in networks. Publicatons Geod. 46.
El-Mowafy, A., Wang, K., 2022. The potential of LEO mega-constellations in aiding GNSS to enable positioning in challenging environments. In XXVII FIG Congress, 1-11.
Ge, M., Gendt, G., Rothacher, M.A., Shi, C., Liu, J., 2008. Resolution of GPS carrier-phase ambiguities in precise point positioning (PPP) with daily observations. J. Geod. 82 (7), 389–399. https://doi.org/10.1007/s00190-007-0187-4.
Gill, E., D'Amico, S., Montenbruck, O., 2007. Autonomous formation flying for the PRISMA mission. J. Spacecr. Rocket. 44 (3), 671–681. https://doi.org/10.2514/1.23015.
Hauschild, A., Tegedor, J., Montenbruck, O., Visser, H., Markgraf, M., 2016. Precise onboard orbit determination for LEO satellites with real-time orbit and clock corrections. In Proceedings of the 29th International Technical Meeting of the Satellite Division of The Institute of Navigation (ION GNSS+ 2016) (3715-3723). https://doi.org/10.33012/2016.14717.
Jäggi, A., Montenbruck, O., Moon, Y., Wermuth, M., König, R., Michalak, G., Bock, H., Bodenmann, D., 2012. Inter-agency comparison of TanDEM-X baseline solutions. Adv. Space Res. 50 (2), 260–271. https://doi.org/10.1016/j.asr.2012.03.027.
Johnston, G., Riddell, A., Hausler, G., 2017. The International GNSS Service. Springer Handbk. Global Navig. Satell. Syst. 967–982. https://doi.org/10.1007/978-3-319-42928-1_33.
Khodabandeh, A., Teunissen, P.J.G., 2015. An analytical study of PPP-RTK corrections: precision, correlation and user-impact. J. Geod. 89, 1109–1132. https://doi.org/10.1007/s00190-015-0838-9.
Lannes, A., Prieur, J.L., 2013. Calibration of the clock-phase biases of GNSS networks: the closure-ambiguity approach. J. Geod. 87, 709–731. https://doi.org/10.1007/s00190-013-0641-4.
Laurichesse, D., Mercier, F., Berthias, J.P., Broca, P., Cerri, L., 2009. Integer ambiguity resolution on undifferenced GPS phase measurements and its application to PPP and satellite precise orbit determination. Navigation 56 (2), 135–149. https://doi.org/10.1002/j.2161-4296.2009.tb01750.x.
Li, B., Ge, H., Ge, M., Nie, L., Shen, Y., Schuh, H., 2019a. LEO enhanced Global Navigation Satellite System (LeGNSS) for real-time precise positioning services. Adv. Space Res. 63 (1), 73–93. https://doi.org/10.1016/j.asr.2018.08.017.
Li, X., Ma, F., Li, X., Lv, H., Bian, L., Jiang, Z., Zhang, X., 2019b. LEO constellation-augmented multi-GNSS for rapid PPP convergence. J. Geod. 93, 749–764. https://doi.org/10.1007/s00190-018-1195-2.
Li, X., Wu, J., Zhang, K., Li, X., Xiong, Y., Zhang, Q., 2019c. Real-time kinematic precise orbit determination for LEO satellites using zero-differenced ambiguity resolution. Remote Sens. (Basel) 11 (23), 1–21. https://doi.org/10.3390/rs11232815.
Lindlohr, W., Wells, D., 1985. GPS design using undifferenced carrier beat phase observations. Manuscr. Geodaet. 10 (4), 255–295.
Lou, L., Liu, Z., Zhang, H., Qian, F., Huang, Y., 2020. TH-2 satellite engineering design and implementation. Acta Geod. Cartogr. Sin. 49, 1252–1264. https://doi.org/10.11947/j.AGCS.2020.20200175.
Mi, X., Zhang, B., Yuan, Y., 2019. Multi-GNSS inter-system biases: estimability analysis and impact on RTK positioning. GPS Solut. 23. https://doi.org/10.1007/s10291-019-0873-8 81.
Mi, X., Zhang, B., Odolinski, R., Yuan, Y., 2020. On the temperature sensitivity of multi-GNSS intra-and inter-system biases and the impact on RTK positioning. GPS Solut. 24, 1–14. https://doi.org/10.1007/s10291-020-01027-5.
Mi, X., Zhang, B., El-Mowafy, A., Wang, K., Yuan, Y., 2023. On the potential of undifferenced and uncombined GNSS time and frequency transfer with integer ambiguity resolution and satellite clocks estimated. GPS Solut. 27 (1). https://doi.org/10.1007/s10291-022-01363-8 25.
Montenbruck, O., Garcia-Fernandez, M., Yoon, Y., Schön, S., Jäggi, A., 2009. Antenna phase center calibration for precise positioning of LEO satellites. GPS Solut. 13, 23–34. https://doi.org/10.1007/s10291-008-0094-z.
Montenbruck, O., Hackel, S., van den Ijssel, J., Arnold, D., 2018. Reduced dynamic and kinematic precise orbit determination for the Swarm mission from 4 years of GPS tracking. GPS Solut. 22 (3). https://doi.org/10.1007/s10291-018-0746-6 79.
Odijk, D., 2000. Improving ambiguity resolution by applying ionosphere corrections from a permanent GPS array. Earth Planets Space 52, 675–680. https://doi.org/10.1186/BF03352262.
Odijk, D., 2002. Fast precise GPS positioning in the presence of ionospheric delays. Publications Geod. 52.
Odijk, D., Zhang, B., Khodabandeh, A., Odolinski, R., Teunissen, P.J.G., 2016. On the estimability of parameters in undifferenced, uncombined GNSS network and PPP-RTK user models by means of *S*-system theory. J. Geod. 90 (1), 15–44. https://doi.org/10.1007/s00190-015-0854-9.
Odijk, D., Khodabandeh, A., Nadarajah, N., Choudhury, M., Zhang, B., Li, W., Teunissen, P.J.G., 2017. PPP-RTK by means of *S*-system theory: Australian network and user demonstration. J. Spat. Sci. 62 (1), 3–27. https://doi.org/10.1080/14498596.2016.1261373.
Odolinski, R., Teunissen, P.J.G., Odijk, D., 2015a. Combined BDS, Galileo, QZSS and GPS single-frequency RTK. GPS Solut. 19, 151–163. https://doi.org/10.1007/s10291-014-0376-6.
Odolinski, R., Teunissen, P.J.G., Odijk, D., 2015b. Combined GPS+ BDS for short to long baseline RTK positioning. Meas. Sci. Technol. 26 (4). https://doi.org/10.1088/0957-0233/26/4/045801 045801.
Psychas, D., Khodabandeh, A., Teunissen, P.J.G., 2022. Impact and mitigation of neglecting PPP-RTK correctional uncertainty. GPS Solut. 26 (1). https://doi.org/10.1007/s10291-021-01214-y 33.
Rebischung, P., Schmid, R., 2016. IGS14/igs14. atx: a new framework for the IGS products. In AGU fall meeting 2016.
Schaer, S., Villiger, A., Arnold, D., Dach, R., Prange, L., Jäggi, A., 2021. The CODE ambiguity-fixed clock and phase bias analysis products: generation, properties, and performance. J. Geod. 95. https://doi.org/10.1007/s00190-021-01521-9 81.
Suesser-Rechberger, B., Krauss, S., Strasser, S., Mayer-Guerr, T., 2022. Improved precise kinematic LEO orbits based on the raw observation approach. Adv. Space Res. 69 (10), 3559–3570. https://doi.org/10.1016/j.asr.2022.03.014.
Teunissen, P.J.G., 1985. Zero order design: generalized inverses, adjustment, the datum problem and S-transformations (11–55). Springer, Berlin Heidelberg.
Teunissen, P.J.G., 1995. The least-square ambiguity decorrelation adjustment: a method for fast GPS integer ambiguity estimation. J. Geod. 70 (1), 65–82. https://doi.org/10.1007/BF00863419.
Teunissen, P.J.G., 2001. Integer estimation in the presence of biases. J. Geod. 75, 399–407. https://doi.org/10.1007/s001900100191.
Teunissen, P.J.G., 2018. Distributional theory for the DIA method. J. Geod. 92 (1), 59–80. https://doi.org/10.1007/s00190-017-1045-7.
Teunissen, P.J.G., 2020. GNSS precise point positioning. position, navigation, and timing technologies in the 21st century: integrated

satellite navigation. Sensor Syst. Civ. Appl. 1, 503–528. https://doi.org/10.1002/9781119458449.ch20.

Teunissen, P.J.G., Khodabandeh, A., 2015. Review and principles of PPP-RTK methods. J. Geod. 89 (3), 217–240. https://doi.org/10.1007/s00190-014-0771-3.

Verhagen, S., Teunissen, P.J.G., 2013. The ratio test for future GNSS ambiguity resolution. GPS Solut. 17, 535–548. https://doi.org/10.1007/s10291-012-0299-z.

Yi, B., Gu, D., Shao, K., Ju, B., Zhang, H., Qin, X., Duan, X., Huang, Z., 2021. Precise relative orbit determination for Chinese TH-2 satellite formation using onboard GPS and BDS2 observations. Remote Sens. (Basel) 13 (21). https://doi.org/10.3390/rs13214487 4487.

Yi, B., Gu, D., Ju, B., Shao, K., Zhang, H., 2022. Enhanced baseline determination for formation flying LEOs by relative corrections of phase center and code residual variations. Chin. J. Aeronaut. 35 (2), 185–194. https://doi.org/10.1016/j.cja.2021.03.016.

Yunck, T., Bertiger, W., Wu, S., Bar-Sever, Y., Christensen, E., Haines, B., Lichten, S., Muellerschoen, R., Vigue, Y., Willis, P., 1994. First assessment of GPS-based reduced dynamic orbit determination on TOPEX/Poseidon. Geophys. Res. Lett. 21 (7), 541–544. https://doi.org/10.1029/94GL00010.

Zehentner, N., Mayer-Gürr, T., 2016. Precise orbit determination based on raw GPS measurements. J. Geod. 90, 275–286. https://doi.org/10.1007/s00190-015-0872-7.

Zha, J., Zhang, B., Liu, T., Hou, P., 2021. Ionosphere-weighted undifferenced and uncombined PPP-RTK: theoretical models and experimental results. GPS Solut. 25 (4). https://doi.org/10.1007/s10291-021-01169-0 135.

Zhang, B., Chen, Y., Yuan, Y., 2019. PPP-RTK based on undifferenced and uncombined observations: theoretical and practical aspects. J. Geod. 93, 1011–1024. https://doi.org/10.1007/s00190-018-1220-5.

Zhang, H., Gu, D., Ju, B., Shao, K., Yi, B., Duan, X., Huang, Z., 2021. Precise orbit determination and Maneuver assessment for TH-2 satellites using spaceborne GPS and BDS2 observations. Remote Sens. (Basel) 13 (24). https://doi.org/10.3390/rs13245002 5002.

Zhang, B., Teunissen, P.J.G., Odijk, D., 2011. A novel un-differenced PPP-RTK concept. J. Navig. 64 (S1), S180–S191. https://doi.org/10.1017/S0373463311000361.

Zhang, B., Hou, P., Zha, J., Liu, T., 2022. PPP–RTK functional models formulated with undifferenced and uncombined GNSS observations. Satell. Navig. 3 (1). https://doi.org/10.1186/s43020-022-00064-4 3.

Zumberge, J., Heflin, M., Jefferson, D., Watkins, M., Webb, F., 1997. Precise point positioning for the efficient and robust analysis of GPS data from large networks. J. Geophys. Res. Solid Earth 102 (B3), 5005–5017. https://doi.org/10.1029/96JB03860.